The Separating Mechanisms in Poincaré Halfmaps

Claus Kahlert and Otto E. Rössler
Institute for Physical and Theoretical Chemistry, University of Tübingen, Tübingen, F.R.G.

Z. Naturforsch. **41 a**, 1369–1380 (1986); received March 20, 1986

The separating mechanisms occuring in a class of Poincaré halfmaps that is induced by the flow of a saddle-focus are described quantitatively. The "critical spiral" is calculated explicitly inside the domain of the map. A complete hierarchy, consisting of three different types of separating mechanisms, is demonstrated. It is characterized in terms of the properties of the critical spiral, as it depends on the canonical parameters of the system.

1. Introduction

The description of two-region piecewise-linear continuous dynamical systems in terms of Poincaré halfmaps arises in a natural manner. A system trajectory is easily found (as a sequence of successive solutions of linear initial value problems) as soon as all its entry or exit points, respectively, of the regions are known [1]. The main problem hereby is, to determine the corresponding exit point for a given entry point, leading to an implicit transcendental equation for each region. The latter equations are representations of halfmaps. If the domain of one halfmap is taken as a Poincaré cross section, the composition of the two halfmaps is an ordinary Poincaré map [2].

Even for rather simple systems, like those possessing only three variables and a flat separating plane in between the two regions, a halfmap induced by the dynamics of a real (i.e., actually present inside the region in question [3]) saddle-focus possesses the capability of separating nearby points. Such a mechanism gives rise to sensitive dependence on initial conditions [4] and implies a fast decay of correlations [5] (which are the characteristics of a chaotic solution).

The separating mechanism in the halfmap to be considered here has to do with a "cutting open" curve, the critical spiral, that intersects a family of invariant curves in such a way that points to the left and to the right of the intersection are mapped far apart from each other. In the case of "complicated isolae" [6, 2] some of the invariant curves are actually cut open *twice*, thereby yielding a disconnected image of a connected set. In addition, a third separating mechanisms, combining the first two, will be described as the most complicated one possible.

As a consequence, *all* topological properties of a halfmap that is induced by the dynamics of a saddle-focus in three space can be indicated. Moreover, explicit or, in some cases, implicit conditions on the canonical parameters for the appearance of the different types of behavior will be presented for the first time.

Reprint requests to Dr. C. Kahlert, Institut für Physikalische und Theoretische Chemie der Universität Tübingen, Auf der Morgenstelle 8, D-7400 Tübingen, F.R.G.

2. Formulation of the Halfmap

For an introduction to the notion of halfmaps see [2]. We use the notation developed there, with some minor modifications. As only the region $\bar{T}$ and the corresponding halfmap $\bar{P}$ will be treated, all the bars on quantities referring to this halfmap will be suppressed. Let us recall the basic equation of motion, stated in diagonalized and gauged form, with canonical parameters $\delta > 0$, $\varrho > 1$, and $\omega > 0$:

$$\mathrm{d}x/\mathrm{d}t = -\varrho x \quad \text{and} \quad \mathrm{d}y/\mathrm{d}t = (1 + i\,\omega)\, y, \qquad x \in \mathbb{R}, \quad y \in \mathbb{C}, \tag{1}$$

where $y =: \eta + i\xi$ ($\eta, \xi \in \mathbb{R}$).

The function

$$u(x, y) := x + 2\,\mathrm{Re}\, y = x + 2\eta \tag{2}$$

corresponds to the first component in the original coordinates of the motivating problem. For brevity we may write its time evolution in the form $u(t)$ instead of $u(x(t), y(t))$. The all important switching condition, defining the separating plane S, is con-

0340-4811 / 86 / 1200-1369 $ 01.30/0. – Please order a reprint rather than making your own copy.

trolled by u alone and reads

$$u(x, y) = x + 2\eta = \delta. \tag{3}$$

Thus every point inside the separating plane can be characterized uniquely by its x- and ξ-coordinate while the value of η is a linear function of x alone:

$$\eta(x) = \frac{\delta - x}{2}. \tag{3a}$$

Hence a point from S can be denoted simply as $(x, \xi)^T$ instead of $(x, \eta(x) + i\,\xi)^T$. In the metric used here [2], (3) motivates the following two definitions:

$$x_0 := \delta \quad \text{and} \quad \eta_0 := \frac{\delta_0}{2}. \tag{5}$$

These are the coordinate values that characterize the static manifolds (see [2], Section 5).

Turning now to the dynamical behavior, any trajectory that contributes to the halfmap $\bar{P}$ has to fulfill the entry and exit condition, respectively, of the region $\bar{T}$, namely:

$$u(0) = u(\tau) = x_0 \tag{6}$$

where τ is the "mapping time", i.e., the span of time after which the switching condition matches again. Hence for any entry point $(x, \xi)^T$ from S^-, the corresponding exit point will be characterized by the right-hand part of (6), i.e., by the implicit equation

$$u(\tau) = x\,e^{-\varrho\tau} + 2\,\mathrm{Re}[(\eta(x) + i\,\xi) \cdot \exp\{(1 + i\,\omega)\,\tau\}] = x_0. \tag{6a}$$

The resulting map is called regular if τ is the first (from countably many) positive solutions of (6a). Equation (6) combined with this latter constraint is the representation of the halfmap to be used in the following.

3. The Partition of the Line W

The boundary between the halfplanes S^+ and S^- is simply a straight line, called W, which can be written as

$$\xi_W(x) = \frac{x_0 - (\varrho + 1)\,x}{2\,\omega}, \tag{7}$$

see [2].

Almost all trajectories passing through a point of this line are tangential to S, i.e., posses an extremum

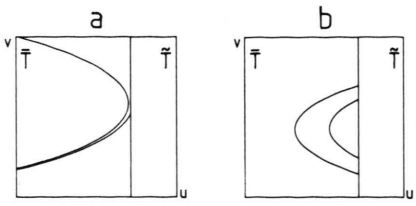

Fig. 1. Schematic plot of the behavior responsible for the separation of adjacent trajectories in a linear partial system. (a) If a u-maximum is present, of two closely adjacent trajectories one may leave the region $\bar{T}$ while the other remains there.– (b) For trajectories with a minimum of the u-component adjacent entry points always lead to nearby exit points.

of the function u that controls the switching of dynamics.

The appearance of a maximum (for the other halfmap: a minimum) in the u-coordinate of the trajectories is responsible for all separating mechanisms. Of two adjacent trajectories possessing their u-maxima at the values $x_0 + \varepsilon$ and $x_0 - \varepsilon$, respectively, the first one fulfills the switching condition at a point of S^+ close to W and thus leaves $\bar{T}$ from there (that is, switches dynamics without actually reaching the maximum), while the second one stays unswitched for another turn around the unstable manifold and therefore exits $\bar{T}$ in a point far from the first orbit (see Figure 1 a).

The character of the flow along W can be determined by calculating the second derivative of u with respect to t on this line:

$$\ddot{u}_W := \left.\frac{\mathrm{d}^2 u}{\mathrm{d}t^2}\right|_W = x\,(\omega^2 + (\varrho + 1)^2) - x_0\,(\omega^2 + 1). \tag{8}$$

Hence a point exists on W, having x-coordinate

$$x_W = x_0\,\frac{\omega^2 + 1}{\omega^2 + (\varrho + 1)^2} \tag{9a}$$

and ξ-coordinate

$$\xi_W(x_W) = \frac{\eta_0}{\omega}\,\frac{\varrho\,(\varrho + 1 - \omega^2)}{\omega^2 + (\varrho + 1)^2}, \tag{9b}$$

at which the curvature of one trajectory vanishes. (Equation (18 b) of [8] is analogous.) Since the point $(x_W, \xi_W(x_W))^T$ is uniquely characterized by its x-coordinate, we shall denote it simply by x_W. It is at this point that the flow of the system changes its character. For x-values greater than x_W, all trajectories possess a *minimum* of their u-component whereas below x_W we find *maxima*. As shown in

Fig. 1, it is only for the latter values of x that the separating property of the halfmap appears.

The behavior of the system at x_W itself is obtained from the third derivative of u at this point, yielding:

$$\left.\frac{d^3u}{dt^3}\right|_{x_W} = -x_0\,\varrho\,(\omega^2+1). \tag{10}$$

The latter quantity cannot vanish for the parameter range admissible ($\varrho > 1$ and x_0, $\omega > 0$ [2]). Therefore x_W is the only point along W where a trajectory possesses no extremum; it is a transversal boundary point [1] and hence an exit point of the region $\bar{T}$.

Together with x_W we have determined the portion of W, to be called W_S, where a separation occurs. As for both $x < 0$ [2] and $x \geqq x_W$ adjacent trajectories are not separated, W_S is characterized by the x-interval $[0, x_W)$. This interval is half-open since the second final point was shown to be a transversal boundary point of $\bar{T}$.

It is of special interest to investigate the roots of $\xi_W(x_W)$ as a function of the parameters ϱ and ω. The only physically meaningful zero is found for

$$\omega^2 = \varrho + 1. \tag{11}$$

This is exactly the criterion for the first appearance of complicated isolae in [2]. Along this curve in parameter space we moreover find

$$x_W = \frac{x_0}{\varrho+1} = x_C\,. \tag{12}$$

Hence x_W coincides with the Cartesian point x_C (see again [2]). The latter property will turn out to be useful for a characterisation of the halfmaps in terms of the critical spiral.

As the last quantity in this Section, let us calculate the pertinent radius of the invariant curve $\Gamma(r_W)$ containing the point x_W. It is found using Eq. (53) of [2] to be

$$r_W = \eta_0 \frac{\varrho}{\omega}\left(\frac{x_W}{x_0}\right)^{(\varrho+2)/2\varrho}. \tag{13}$$

The latter result shows what kinds of invariant curves Γ are subject to a separating mechanism: Only for those that intersect W_S does a separation occur (while for all the others the halfmap acts more or less as a reflection along W). Specifically for $\omega^2 < \varrho + 1$, we find $r_W > r_C$ (see Eq. (64) of [2]). Hence all base lines, the Cartesian leaf, as well as a fraction of the Ω-curves intersect W_S (see [2], Figure 8). In contrast, for $\omega^2 > \varrho + 1$, the base lines and a portion of the isolae along with the Cartesian leaf all have points in common with W_S. The separation in this case therefore no longer affects any Ω-curve. Instead, some of the invariant curves intersect W_S twice (see [2], Fig. 7), first with their base line portion and a second time with the corresponding (complicated) isola. These curves are mapped in a more complicated fashion.

4. The Critical Spiral

A separation appears, as we saw, when of two adjacent trajectories, one leaves the region $\bar{T}$ while the other stays over. In between, a trajectory exists with a maximum of the u-coordinate, which occurs exactly at $u = x_0$. This kind of orbit is called touching or osculating since it possesses a point of contact with the separating plane S. At the entry points of touching trajectories the mapping time and hence the halfmap itself behaves discontinuously, thus they form a branch cut in the sense of the theory of functions (cf. e.g. [9]). At those points, not only (6a) but also

$$\left.\frac{du}{dt}\right|_S = -\varrho\,x\,e^{-\varrho\tau} + 2\,e^{\tau}[(\eta(x) - \omega\,\xi)\cos\omega\,\tau - (\omega\,\eta(x) + \xi)\sin\omega\,\tau] = 0 \tag{14}$$

has to be fulfilled.

Our task is to calculate the geometric locus of these entry points. Since (6a) cannot be solved analytically as it stands, solving it simultaneously with (14) is not possible either. We are going to tackle this task as an inverse problem. An appropriate procedure was worked out in [7, 8].

Let us apply the formalism indicated there. First, we have to find the curves of equal mapping time:

$$\xi_\tau(x) = \frac{e^{-(\varrho+1)\tau} - \cos\omega\,\tau}{2\sin\omega\,\tau}\,x - \frac{e^{-\tau} - \cos\omega\,\tau}{2\sin\omega\,\tau}\,x_0. \tag{15}$$

In the present case these curves are simply straight lines inside the separating plane S.

To further investigate the family of functions ξ_τ, let us treat the limiting behavior for $\tau \to 0$. In this case (15) yields an undefined expression of

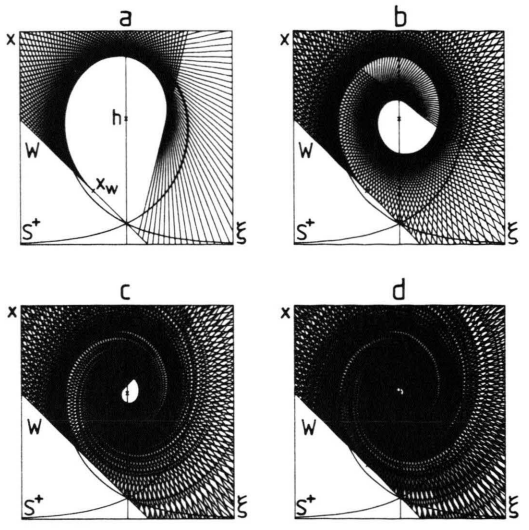

Fig. 2. Lines of equal mapping time $\xi_\tau(x)$, restricted to S^-. If $\Delta\tau$, the difference between subsequent τ-values, is small, the intersections of these lines virtually coincide with entry points of touching trajectories. Four τ-intervals are shown with an increment $\Delta\tau = 0.01$: (a) $\tau = 0 \ldots 1$ (100 lines); (b) $\tau = 0 \ldots 2$ (200 lines); (c) $\tau = 0 \ldots 3$ (300 lines); (d) $\tau = 0 \ldots 4$ (400 lines). Parameters: $x_0 = 1$, $\varrho = 5$, $\omega = 5$. Axes: $x = 0 \ldots 1.7$, $\xi = -0.5 \ldots 0.5$.

the form "0/0" in both terms. It can be made regular by applying l'Hospital's rule, however, so that

$$\xi_0(x) := \lim_{\tau \to 0} \xi_\tau(x) = -\frac{\varrho + 1}{2\omega} x + \frac{\eta_0}{\omega}, \qquad (16)$$

giving us back the equation for W. This result makes sense: As the mapping time approaches zero, an entry point of $\bar{T}$ necessarily has to coalesce with its corresponding exit point – and only along W the trajectories are tangential to S.

Calculating now the x-components of the intersection points of the lines $\xi_\tau(x)$ and $\xi_{\tau+\Delta\tau}(x)$ and taking the limit $\Delta\tau \to 0$ properly [8], we find for the "numerator and denominator functions" z and n, respectively:

$$z(\tau) = -\omega + e^{-\tau}(\omega \cos \omega\tau + \sin \omega\tau) \qquad (17a)$$

and

$$n(\tau) = -\omega + e^{-(\varrho+1)\tau} \cdot (\omega \cos \omega\tau + (\varrho + 1) \sin \omega\tau). \qquad (17b)$$

Compared to analogous expressions in [8], we find only different signs of τ, apart from the fact that in z also a change in the sign of the leading ω-term occurs. These two changes are responsible

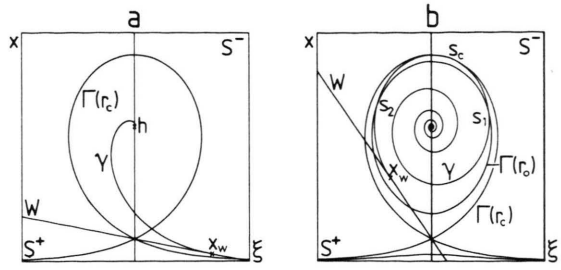

Fig. 3. The analytically obtained critical spiral γ. Also shown is the Cartesian leaf $\Gamma(r_C)$. (a) For parameters fulfilling $\omega^2 < \varrho + 1$, the spiral starts outside the Cartesian leaf and intersects all three types of invariant curves, including Ω-curves, exactly once. Parameters: $x_0 = 1$, $\varrho = 5$, $\omega = 1$. Axes: $x = 0 \ldots 1.7$, $\xi = -0.5 \ldots 0.5$. (b) If ω^2 becomes greater than $\varrho + 1$, the initial point of the spiral, x_W, is located on an isola and γ runs completely inside the Cartesian leaf intersecting the complicated isola $\Gamma(r_0)$ twice. Parameters: $x_0 = 1$, $\varrho = 5$, $\omega = 7.5$, $r_0 = 0.9\, r_C$. Axes: $x = \ldots 1.7$, $\xi = -0.5 \ldots 0.5$

for the existence (in the present case) and the nonexistence (in the other) of the limits $\tau \to 0$ and $\tau \to \infty$, as we proceed to show.

The lemma proved in the Appendix shows that both functions z and n have their only nonnegative zero at the origin. So the quotient $z(\tau)/n(\tau)$ remains finite for $\tau > 0$ and hence yields a well defined analytical expression for the x-components investigated, namely:

$$x_\tau := x_0 \frac{z(\tau)}{n(\tau)}. \qquad (18)$$

The corresponding ξ-components are obtained by inserting x_τ into (15). This means that for every $\tau > 0$, we find an entry point of a touching trajectory explicitly, as

$$\gamma(\tau) := (x_\tau, \xi_\tau(x_\tau))^T. \qquad (19)$$

This is the first main result of the present paper: We have obtained a parametric representation of the critical spiral [6] γ in the (system independent) (x, ξ)-representation of the separating plane. Figure 3 illustrates this result and its main consequences (to be discusses further in Sections 5 and 6).

As a corollary, it is of interest that from our possessing explicit knowledge of the critical spiral itself, we can also indicate the image points of this curve explicitly. Before doing this, we first have to say what we mean by the "image" of the critical spiral, because along this curve the halfmap behaves discontinuously.

Since at a point of contact the switching condition (6) is fulfilled as well as at an exit point, we may add W_S (containing simultaneous exit and reentry points of $\bar{T}$) to the domain and to the range of the halfmap $\bar{P}$. On the one hand, approaching the spiral along an isola in a counter-clockwise manner yields a point located on W_S. On the other hand, the "true" exit points of trajectories starting on γ are to be found for the "clockwise limit". These latter points can be called the image of W_S. (They will be investigated in [11].)

Now it is easy to determine the image of γ. For any point of the spiral, we already know the mapping time τ. Therefore we find

$$\bar{P}(\gamma(\tau)) = (x_\tau e^{-\varrho\tau}, \xi_W(x_\tau e^{-\varrho\tau}))^{\mathrm{T}}. \tag{20}$$

Since the image of γ is located on W_S, we may again characterize these points by their x-coordinate alone, and denote this quantity as

$$x_S(\tau) := x_\tau e^{-\varrho\tau}. \tag{20a}$$

This function will play a key role in investigating the critical spiral.

5. The Properties of the Critical Spiral

Now that we know the critical spiral explicitly, let us look at its properties, first the limiting behavior for $\tau \to 0$ and $\tau \to \infty$, respectively. In the former case, we find that z and n both vanish quadratically as their arguments tend towards zero. The limit can, however, again be taken regularly (see also the Appendix), yielding

$$\lim_{\tau \to 0} x_\tau = x_W. \tag{21}$$

The other limiting case, $\tau \to \infty$, is found immediately:

$$\lim_{\tau \to \infty} x_\tau = x_0 \quad \text{and} \quad \lim_{\tau \to \infty} \xi_\tau(x_0) = 0. \tag{22}$$

This point is nothing but the homoclinoid point h discussed in [2] – the only entry point with an associated infinite mapping time.

Now that we have determined the final and initial point of the critical spiral, let us investigate the range in between. We shall discuss it in polar coordinates, using the "natural geometry" of the separating plane, i.e., taking the invariant curves as "circles" [2].

The property of highest interest is the momentary radius r_γ of the critical spiral. Here we find, in analogy to what we did in (13) above,

$$r_\gamma^2(\tau) := [\eta^2(x_\tau) + \xi_\tau^2(x_\tau)] \left(\frac{x_\tau}{x_0}\right)^{2/\varrho}. \tag{23}$$

This expression, as given, does not yield much information about the structure of the critical spiral as yet. To obtain a better insight, we change from the mapping time "τ-representation" to the geometric "x-representation" of the problem. (Implicitly we shall, however, think about the spiral as running from x_W to h, i.e., in the direction of growing τ-values.) Since the radial coordinate of a point remains invariant under the action of a halfmap, as far as the radius is concerned, we can investigate the image of γ rather than the spiral itself – provided the halfmap acts in a one-to-one manner on the spiral. (A criterion for that to happen will be given shortly. We shall assume this property to hold true for the rest of this Section.)

Let us now turn to a concrete x-representation of r_γ. The radius function of W_S is found in analogy to (23):

$$r_\gamma(x) = \sqrt{\eta^2(x) + \xi_W^2(x)} \left(\frac{x}{x_0}\right)^{1/\varrho} = \frac{x_0}{2\omega} \sqrt{\left(\frac{x}{x_0}\right)^2 (\omega^2 + (\varrho+1)^2) - 2\left(\frac{x}{x_0}\right)(\omega^2 + \varrho + 1) + (\omega^2+1)} \left(\frac{x}{x_0}\right)^{1/\varrho}, \tag{24}$$

The corresponding ξ-component becomes $\xi_W(x_W)$. Thus the starting point of the critical spiral is the end point of W_S. This result could have been anticipated: As the mapping time goes towards zero, the entry point of a touching trajectory is bound to coalesce with its point of contact.

Now the decisive question to be treated concerns the extrema of the radius. To obtain them we have to determine the derivative of the radius,

$$\frac{\mathrm{d}}{\mathrm{d}x} r_\gamma(x) = \frac{1}{2 r_\gamma(x)} \frac{x_0}{2\omega^2 \varrho} \left(\frac{x}{x_0}\right)^{(2-\varrho)/\varrho} R\left(\frac{x}{x_0}\right), \tag{25}$$

where

$$R\left(\frac{x}{x_0}\right) := \left(\frac{x}{x_0}\right)^2 (\varrho+1)\,(\omega^2+(\varrho+1)^2) - \left(\frac{x}{x_0}\right)(\varrho+2)\,(\omega^2+\varrho+1) + (\omega^2+1). \tag{25a}$$

The latter function possesses its zeros at

$$\left(\frac{x}{x_0}\right)_1 = \frac{1}{\varrho+1} \quad \text{and} \quad \left(\frac{x}{x_0}\right)_2 = \frac{\omega^2+1}{\omega^2+(\varrho+1)^2}. \tag{26}$$

This shows that the extrema of r_γ are located at the already well known values x_C and x_W, respectively. (See Eq. (65) of [2] for the former and (9a) for the latter.) The first extremum is of interest only if $x_W > x_C$, otherwise x_C is not located inside W_S. By contrast, the second extremum coincides with the initial point of the critical spiral (and its image). This means that the spiral, for all values of the canonical parameters, starts out tangentially to $\Gamma(r_W)$.

In order to determine the character of the two extrema, we calculate the second derivative of r_γ:

$$\frac{d^2}{dx^2} r_\gamma(x) = \frac{1}{2 r_\gamma(x)} \frac{x_0}{2\omega^2\varrho} \left(\frac{x}{x_0}\right)^{2(1-\varrho)/\varrho} \cdot \left[\frac{2-\varrho}{\varrho x_0} R\left(\frac{x}{x_0}\right) + \left(\frac{x}{x_0}\right) \frac{d}{dx} R\left(\frac{x}{x_0}\right)\right] - \frac{1}{2 r_\gamma^2(x)} \frac{d}{dx} r_\gamma(x). \tag{27}$$

Since in (27) the product in front of the square brackets is certainly positive, and since both R and the term in the third line vanish at the two points of interest, it suffices to look at the derivative of the function R at these points:

$$V(x) := \frac{d}{dx} R\left(\frac{x}{x_0}\right) = \frac{1}{x_0}\left[2\left(\frac{x}{x_0}\right)(\varrho+1) \cdot (\omega^2+(\varrho+1)^2) - (\varrho+2)\,(\omega^2+\varrho+1)\right]. \tag{28}$$

Inserting for x the values x_C and x_W, respectively, gives

$$V(x_C) = \frac{1}{x_0}(\varrho+1-\omega^2)$$

and

$$V(x_W) = \frac{1}{x_0}(\omega^2-\varrho-1) = -V(x_C). \tag{28a}$$

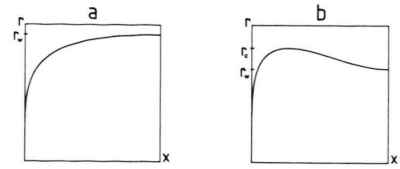

Fig. 4. Two types of behavior of the radius function of γ. (a) If $\omega^2 < \varrho+1$, we find a strictly monotonic behavior of r_γ, from zero up to its final value r_W. (b) For $\omega^2 > \varrho+1$ the radius function possesses a maximum of value r_C in the outermost turn of the spiral. Parameters for (a): $x_0 = 1$, $\varrho = 5$, $\omega = 1$. Parameters for (b): $x_0 = 1$, $\varrho = 5$, $\omega = 7.5$. Axes: $x = 0 \ldots x_W$, $r = 0 \ldots 1.2\, r_C$.

This shows that for $\omega^2 < \varrho+1$, the function r_γ possesses its only local extremum (a maximum) at x_W. (The extension of r_γ beyond x_W incidentally shows a local minimum at the point x_C, which, however, lies outside of W_S in the present case.) Therefore the radius of the critical spiral is found to monotonically decrease from the value r_W at x_W, down to 0 at h.

When $\omega^2 = \varrho+1$, the two points x_C and x_W coincide. And beyond this curve in parameter space, x_W becomes greater than x_C. In this case the signs of $V(x_W)$ and $V(x_C)$ are interchanged as compared to the first one, so r_γ possesses a local minimum at x_W and a local maximum at x_C (the latter being an absolute maximum). This means that in the outermost turn of the critical spiral the radius at first increases, until it reaches the value r_C (see Eq. (64) of [2]) – which is the characteristic radius of the Cartesian leaf – in order to thereafter strictly decrease. Thus whenever a complicated isola is present, γ touches $\Gamma(r_C)$ in the preimage of the Cartesian point x_C.

Before turning to the dynamical aspects of the critical spiral, let us look at a "corollary" that directly follows from the extremum property of r_γ at x_W: *One particular invariant curve, $\Gamma(r_W)$, touches W in the point x_W.*

To prove this, we have to look at the extension of r_γ beyond x_W: The point x_W is certainly located on $\Gamma(r_W)$, cf. (13). Let us assume that $\Gamma(r_W)$ *intersects* W in x_W; then for *all* $\varepsilon > 0$ and $\varepsilon' > 0$ below an upper bound Δ, the two points of W with x-coordinates $x_W + \varepsilon$ and $x_W - \varepsilon'$, respectively, must be situated inside and outside of the "circle" $\Gamma(r_W)$. Thus these points belong to different invariant curves with radii less and greater than r_W. On the other hand, the extension of r_γ possesses a local extremum at x_W, therefore we can choose $\varepsilon > 0$ and

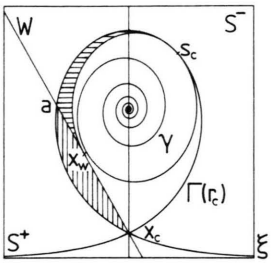

Fig. 5. Mode of action of the halfmap if $\omega^2 > \varrho + 1$. The horizontally hatched "triangle" (x_W, s_C, a) is mapped onto the vertically hatched interior of the Cartesian leaf inside S^+. The portion of W with $x > x_W$ consists of fixed points of the halfmap, therefore the arc $\overset{\frown}{a s_C}$ of $\Gamma(r_C)$ is mapped onto $\overset{\frown}{a x_C}$, and the portion $\overset{\frown}{x_W s_C}$ of γ is mapped onto the "interval" (x_W, x_C) of W_S. Parameters: $x_0 = 1$, $\varrho = 5$, $\omega = 9$. Axes: $x = 0 \ldots 1.7$, $\xi = -0.5 \ldots 0.5$.

$\varepsilon' > 0$ (below Δ) to obtain $r_\gamma(x_W - \varepsilon') = r_\gamma(x_W + \varepsilon)$. This is a contradiction to the assumption mode. Hence the point x_W cannot be an intersection point of $\Gamma(r_W)$ with W; rather, since it is from W, it has to be a *point of contact*. From the corollary follows that complicated isolae (being capable of crossing W) are characterized by a radius r_0 that is greater than r_W.

The findings of the present Section about the critical spiral now finally yield a coherent dynamical picture for the second separating mechanism, as is illustrated in Figure 5. There the horizontally hatched portion of the halfplane S^- in between the critical spiral and the Cartesian leaf, representing points of complicated isolae, is "mirrored" onto the vertically hatched portion of S^+ in between the Cartesian leaf and W. Hereby the arc $\overset{\frown}{a s_C}$ of $\Gamma(r_C)$ is mapped onto the arc $\overset{\frown}{a x_C}$; and the arc $\overset{\frown}{x_W s_C}$ of γ is mapped onto the "interval" (x_W, x_C) of W. Note that the point s_C (the point of contact between $\Gamma(r_C)$ and γ) is mapped to x_C. The rest of the interior of the Cartesian leaf is mapped into the region of the base lines. This picture shows *quantitatively* how the image of a connected set inside the halfplane S^- becomes disconnected under the action of the halfmap.

6. The "Folding" of the Critical Spiral

As the radius function r_γ may first be growing in the outermost turn of the critical spiral (Fig. 4b), in order to thereafter decrease monotonically, the possibility of a *self-intersection* of the spiral arises. If this happens in a point $\gamma(\tau)$, we necessarily find a second associated mapping time $\tau' > \tau$, such that

$$\gamma(\tau') = \gamma(\tau). \tag{29}$$

A trajectory starting at this point touches S twice, both after time τ and again after τ'. Hence it is a "doubly touching trajectory" (cf. [6]). Two is already the maximum number of points of contact with S possible for any trajectory since none of the invariant curves can intersect W_S more than twice; for a proof see [7]. Doubly touching trajectories give rise to a *third* separating mechanism of the halfmap, which then is the most complicated one.

A self-intersection of the spiral occurs when its radius possesses the same magnitude twice, at phases that differ by an integer multiple of 2π. Since the radius function reaches its maximum possible value, r_C, in the outermost turn of the spiral, a point of self-intersection can only occur if at the end of this turn r_γ exceeds r_W. In this case γ crosses W and part of it is located inside S^+. Thus the two conditions for a self-intersection of the critical spiral to occur and for its leaving S^-, coincide. (This situation will be encountered again in Fig. 8 below.)

As mentioned already, a self-intersection point of γ is an entry point of a doubly touching trajectory. The second point of contact of such an orbit, being located on W_S too, necessarily possesses two preimages. The first of these is $\gamma(\tau)$ itself (with associated mapping time τ'), the second preimage is the first point of contact (with mapping time $\tau' - \tau$).

This latter point has to be both from γ and from W_S, hence it is the intersection of these curves (the exit point of γ from S^-). Since at least one point has been shown to possess two antecedents, the mapping from the critical spiral onto W_S can no longer be inverted globally. This means that we have to be careful about our arguments using the function r_γ. If γ is no longer mapped one-to-one onto W_S, the graph of r_γ may become more complicated. This problem will be resolved by the selection rules to be introduced below.

The function x_S (which essentially is the halfmap applied to γ) was found to become noninvertible for the case of a critical spiral being capable of self-intersection and hence of crossing W. To see that this condition for noninvertibility is both sufficient and necessary, we calculate two closely related

quantities: Firstly so the derivative of x_S, namely

$$D_1(\tau) := \frac{\mathrm{d}}{\mathrm{d}\tau} x_S(\tau) = \frac{x_0 e^{-\varrho\tau}}{n(\tau)^2} \cdot \left[n(\tau) \left(-\varrho z(\tau) + \frac{\mathrm{d}}{\mathrm{d}\tau} z(\tau) \right) - z(\tau) \frac{\mathrm{d}}{\mathrm{d}\tau} n(\tau) \right]$$

$$= -\frac{x_0 e^{-\varrho\tau}}{n(\tau)^2} [\varrho\omega(1 + e^{-(\varrho+2)\tau}) - e^{-\tau}((\omega^2 + \varrho + 1)\sin\omega\tau + \varrho\omega\cos\omega\tau) + e^{-(\varrho+1)\tau}((\omega^2 + \varrho + 1)\sin\omega\tau - \varrho\omega\cos\omega\tau)]. \quad (30)$$

Secondly using (1), we calculate the t-derivative of the function u, evaluated at the points of the critical spiral:

$$D_2(\tau) := \frac{\mathrm{d}}{\mathrm{d}t} u(x_\tau, \eta(x_\tau) + i\,\xi_\tau(x_\tau))$$

$$= \frac{x_0}{n(\tau)} [\varrho\omega(1 + e^{-(\varrho+2)\tau}) - e^{-\tau}((\omega^2 + \varrho + 1)\sin\omega\tau + \varrho\omega\cos\omega\tau) + e^{-(\varrho+1)\tau}((\omega^2 + \varrho + 1)\sin\omega\tau - \varrho\omega\cos\omega\tau)]. \quad (31)$$

Comparing (30) and (31), one sees that

$$\frac{D_1(\tau)}{D_2(\tau)} = \frac{-\omega e^{-\varrho\tau}}{n(\tau)} \quad (32)$$

is a positive quantity for all $\tau > 0$. Thus, the u-component (being "perpendicular" to S) of the velocity field at a point of γ determines the derivative of x_S.

Expression (32) thus reveals the existence of a similarity between the dynamics of the critical spiral in the separating plane on the one hand, and the focal motion of trajectories in three-space on the other. A second result implicit in (32) is even more important: Both functions, D_1 and D_2, obtain their zeros simultaneously. Since the u-component of the velocity field vanishes along W, D_1 too becomes zero *only* for points of the critical spiral located on W. Hence x_S is one-to-one as long as γ stays completely inside S^-. Only for values of the parameters ϱ and ω that allow the critical spiral to cross W, does a nonuniqueness of the inverse of x_S appear. This shows that the three conditions, (a) for a self-intersection of the critical spiral, (b) for an intersection of γ with W, and (c) for a not globally invertible image of the spiral under the action of the halfmap, are all mutually equivalent.

Therefore we can determine the boundary inside the canonical parameter space separating those systems that possess a one-to-one image of γ from the rest. The boundary in parameter space is reached when the critical spiral touches W after exactly one turn to revisit its initial point x_W. In this case D_1 possesses there a local maximum of magnitude zero. The conditions to be fulfilled in order for this to happen are

$$D_1(\tau) = 0 \quad (33\,\mathrm{a})$$

and

$$\frac{\mathrm{d}}{\mathrm{d}\tau} D_1(\tau) = 0, \quad (33\,\mathrm{b})$$

respectively.

The expression valid for D_1 was already given (30). Since there the first factor on the right-hand side is strictly positive for $\tau > 0$, we can omit it and obtain from (33 a) a "first partial limiting condition" for the appearance of a self-intersection of the critical spiral:

$$0 = \varrho\omega - e^{-\tau}((\omega^2 + \varrho + 1)\sin\omega\tau + \varrho\omega\cos\omega\tau) + e^{-(\varrho+1)\tau}((\omega^2 + \varrho + 1)\sin\omega\tau - \varrho\omega\cos\omega\tau) + \varrho\omega e^{-(\varrho+2)\tau}. \quad (34)$$

Rather than calculating $\mathrm{d}D_1(\tau)/\mathrm{d}\tau$ in (33 b) directly, we first use (33 a) to simplify it, in order then to obtain the "second partial limiting condition"

$$0 = \frac{\mathrm{d}}{\mathrm{d}\tau} D_1(\tau) + \left(\varrho + \frac{2}{n(\tau)} \frac{\mathrm{d}}{\mathrm{d}\tau} n(\tau) \right) D_1(\tau)$$

$$= \frac{x_0 e^{-\varrho\tau}}{n(\tau)^2} \left[n(\tau) \frac{\mathrm{d}^2}{\mathrm{d}\tau^2} z(\tau) - z(\tau) \frac{\mathrm{d}^2}{\mathrm{d}\tau^2} n(\tau) - \varrho \frac{\mathrm{d}}{\mathrm{d}\tau} (n(\tau) z(\tau)) \right]. \quad (35)$$

Here the first factor stays regular for all $\tau > 0$; so it yields no contribution to condition (33 b). The same holds true for a common factor $\omega e^{-\tau}$. Hence the second partial condition for the appearance of a self-intersecting critical spiral reads

$$0 = (\omega^2 + 1)[\omega\cos\omega\tau - (\varrho + 1)\sin\omega\tau] - e^{-\varrho\tau}(\omega^2 + (\varrho + 1)^2)[\omega\cos\omega\tau - \sin\omega\tau] + e^{-(\varrho+1)\tau}\varrho\omega(\varrho + 2). \quad (36)$$

The conditions (33 a, b), or equivalently (34) and (36), are two transcendental equations in three un-

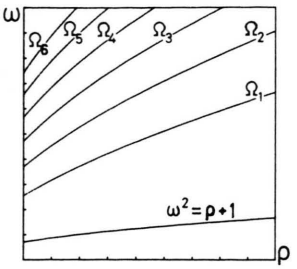

Fig. 6. The first six Ω_n curves, marking the onset of the n-th self-intersection of the critical spiral. For comparison, the curve $\omega^2 = \varrho + 1$ is also shown. Axes: $\varrho = 1 \ldots 10$, $\omega = 0 \ldots 20$.

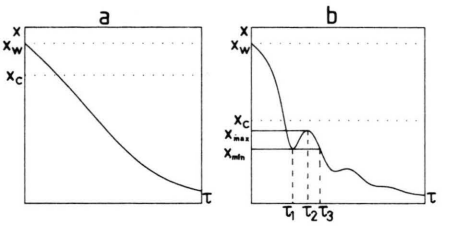

Fig. 7. The image of the critical spiral – only the x-component, the function x_S is shown. (a) For all parameters lying below the curve Ω_1 (cf. Fig. 6), the function x_S is strictly decreasing and hence globally invertible. Parameters: $x_0 = 1$, $\varrho = 5$, $\omega = 2$. Axes: $\tau = 0 \ldots 3$, $x = 0 \ldots 1.1\, x_W$. (b) For parameters above Ω_1, the spiral is mapped onto W_S in a folded (noninvertible) manner. Since only the smallest τ that generates a given x-value contributes to the halfmap, the interval $[\tau_1, \tau_3)$ (and at least one further such interval) have to be cut out from the domain of x_S in order to make the map one-to-one in accordance with the dynamics. Parameters: $x_0 = 1$, $\varrho = 1$, $\omega = 9$. Axes: $\tau = 0 \ldots 3$, $x = 0 \ldots 1.1\, x_W$.

knowns ϱ, ω, and τ. After solving for the parameter of representation, τ, these conditions yield a scalar relation between ϱ and ω. This relation plays a role similar to $0 = \omega^2 - \varrho - 1$ (11). In contrast to the latter, however, which is given in explicit form, (33) is an implicit equation and has to be solved for numerically due to its algebraic complexity. Doing this, one finds that the equation possesses a countable infinity of solutions – curves Ω_n in canonical parameter space (the first six of which are shown in Figure 6). The very first of these curves, Ω_1, yields the boundary between those systems (points in parameter space) which possess a globally invertible image of the critical spiral, and those which do not. The other (higher) solutions, Ω_n ($n = 2, 3, \ldots$), are conditions on the parameters for the n-th self-intersection of γ.

If the critical spiral is not mapped monotonically (one-to-one) onto W_S, it is said to be "folded:". This choice of terminology is motivated by Figure 7. It turns out that the number of folds present for any parameter vector $(\varrho, \omega)^T$ is easy to determine: Just count how many Ω_n curves (Fig. 6) lie below that point.

We are now in the position to discuss the consequences that a folded spiral has on the action of the halfmap. In principle, any noninvertible mapping of γ onto W_S implies a conflict with the uniqueness of trajectories. As it turns out, this problem can be overcome by introducing specific selection rules. To obtain these rules we recall the fact that the representation (19) of γ was found by *neglecting* the switching of the dynamics. This means that after the mapping time τ, the trajectory starting at $\gamma(\tau)$ not necessarily fulfills the switching condition (3) for the *first* time – a property which, however, is requisite for the halfmap.

Nevertheless: *As long as the whole critical spiral stays inside the halfplane* S^-, (3) *is fulfilled for the first time at* τ, *for any entry point* $\gamma(\tau)$. To prove this statement, we assume that a mapping time $0 < \tau' < \tau$ exists for some point of the critical spiral. Then the switching condition for the trajectory starting at this point is fulfilled after a period τ' (leading to an exit point of $\bar{T}$ located inside of S^+). Since we originally assumed a homogeneous dynamics, the trajectory starting at this point eventually touches the separating plane after another specific period of time, $\tau - \tau'$. The exit point mentioned is thus an initial point of a touching trajectory and hence must be a point of the critical spiral. This is a contradiction to the assumption that γ is located completely inside S^-. Thus in the present case, when the critical spiral stays completely inside of S^-, all points of γ contribute to the halfmap. We moreover have obtained a link between the properties of the critical spiral and the question of a regular mapping.

Next, let us see what happens when the critical spiral crosses W and hence possesses points inside S^+. A trajectory starting at a point $\gamma(\tau)$ in the latter halfplane at first has to run inside the region $\tilde{T}$ under the dynamics of $\bar{T}$ in order then to enter $\bar{T}$ in another (regular) point of γ and eventually touch S after time τ. This behavior is obviously irregular from the point of view of the halfmap $\bar{P}$ considered. Therefore, the points of γ located inside S^+ *cannot* yield any contribution to the halfmap.

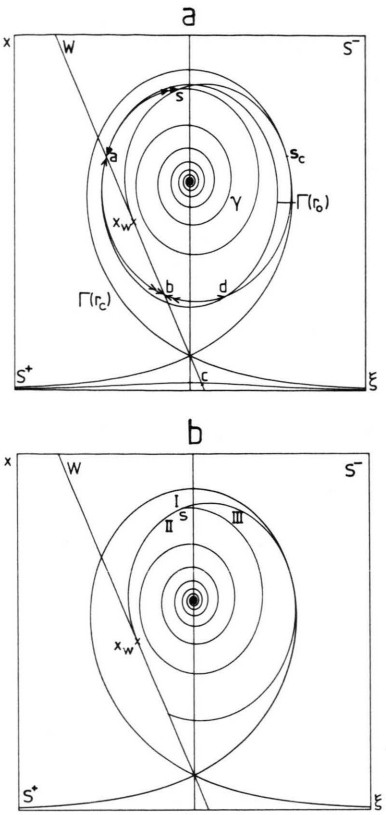

Fig. 8 (a). The behavior of a "folded" (self-intersecting) critical spiral. The arc $\widehat{as}$ (lying in between the reentry and the self-intersection point of the spiral) is mapped onto $\widehat{ab}$ located inside of S^+. Hence neither of these two arcs contributes to the separating mechanisms of the halfmap. (Note that the spiral touches the Cartesian leaf in s_C and intersects the isola $\Gamma(r_0)$ in a and d. This shows that $\widehat{ab}$ is mapped in an "irregular" manner onto the regular segment $\widehat{db}$ of γ.) (b) The same spiral, with the irregular segments ($\widehat{as}$ and $\widehat{ab}$) removed. At the self-intersection point s, three regions (I, II, and III) meet. Traversing the spiral from region I towards II, or from I to III, respectively, we observe the second separating mechanism. Upon crossing the spiral from region II towards III, however, type I separation applies. Parameters for (a) and (b): $x_0 = 1, \varrho = 5, \omega = 12$. Axes: $x = 0 \ldots 1.7, \xi = -0.5 \ldots 0.5$.

It is also easy to see that the portion of the critical spiral in between the reentry point into S^- (point a in Fig. 8) and the (next) point of self-intersection (s) *also* does not contribute to a separating mechanism. This follows from the fact that all the reentry points of γ into S^- by (32) possess x-values greater than x_W, i.e., are located outside W_S. Thus the arc $\widehat{as}$ is just "mirrored" onto the portion of the critical spiral located inside S^+ – that is, onto the arc $\widehat{ab}$. (For entry points from $\widehat{as}$ the exit condition indeed is fulfilled at a $0 < \tau' < \tau$, in a point of S^+.) This means that the two portions of the spiral mentioned ($\widehat{as}$ and $\widehat{ab}$) do not generate regularly touching trajectories. Therefore they must *be cut out* in order to obtain a coherent picture of the halfmap.

To visualize this situation from a different point of view, recall the behavior of the function x_S: When the spiral crosses W_S, the graph of x_S possesses a local minimum ($x_{\min}$); a local maximum ($x_{\max}$) is found for the corresponding reentry point. (It suffices to discuss the situation for the first fold; for the others, if any are present, the arguments are the same.) Inside the interval $(x_{\min}, x_{\max})$ one sees from Fig. 7 that three values of τ lead to the same x-value. So the map cannot be inverted uniquely in this interval. However, only the smallest of these τ's yields a contribution to the halfmap. The two others belong to trajectories running partially inside the region $\tilde{T}$ under the dynamics of $\bar{T}$ – as discussed above. Hence the rising, and falling, segments of x_S correspond to the portion of γ inside S^+ and the portion between the reentry and the self-intersection point, respectively. Thus we have determined the τ-interval $[\tau_1, \tau_3)$ that has to be cut out from the domain of x_S in order to make this map one-to-one in accordance with the switching dynamics.

Finally let us discuss how the folding of γ affects the separating properties of the halfmap. Formerly, the separation of points could always be related to a boundary *curve*, the critical spiral. Points of the halfplane S^- located on different sides of this curve were mapped either to opposite ends of the same region (type I separation) or even into two disconnected regions (type II separation). This time, when we look at the neighborhood of a self-intersection point of γ, we find three different regions (I, II, and III in Fig. 8 b) to be present. Crossing the pertinent arcs of the critical spiral separating these regions, we find type II separation for adjacent points stemming from the first and the second region, as well as for points from the first and the third region. In contrast, adjacent points located inside the second and the third region, respectively, are separated by the first mechanism. Thus by successfully unfolding the type III separation, we have found that it represents a combination of the first two mechanisms, described previously [2].

By virtue of the fact that no triply touching trajectories exist, this third mechanism of separating

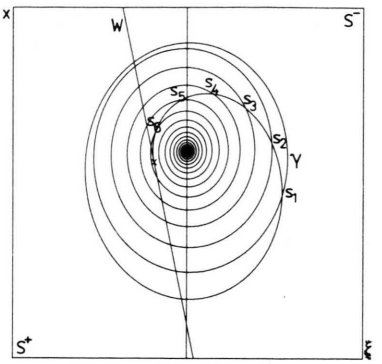

Fig. 9. Example of a critical spiral exhibiting 6 self-intersections (at the points s_1 to s_6). Parameters: $x_0 = 1$, $\varrho = 5$, $\omega = 25$. Axes: $x = 0 \ldots 1.7$, $\xi = -0.5 \ldots 0.5$.

neighboring points is already the most complicated one possible. It nevertheless at the same time generates a new, infinite hierarchy based on the number of self-intersection points of the critical spiral present, cf. Figure 9.

7. Discussion

Two-region piecewise-linear continuous dynamical systems with three variables are the simplest class possessing chaotic solutions. A description of these systems in terms of Poincaré halfmaps comes naturally and is adequate. In general, halfmaps are represented implicitly, and only for exceptional points can their action be written down explicitly. As it happens, the separating mechanisms responsible for the appearance of chaos through a sandwich map mechanism [10] can be described analytically in an explicit fashion.

Three separating mechanisms could be distinguished and derived from the properties of the critical spiral for a halfmap induced by the flow of a 3-D saddle focus. The *first* one (type I) is the one to be expected intuitively – it is found for all values of the parameters. An invariant curve, e.g. an isola, is cut open at its only intersection point with the critical spiral and mapped as a connected arc into the corresponding base line.

The *second* mechanism (type II), as described qualitatively before in [2], appears together with and effects the so-called complicated isolae. It exists above the curve $\omega^2 = \varrho + 1$ in parameter space. Such an isola (more exactly, its part inside S^-) is mapped partially onto the arc inside S^+ and partially into the corresponding base line inside the same halfplane. The boundary in between these portions of the isola is the second point of intersection with the critical spiral (point s_2 in Fig. 3b; this point is mapped to the intersection of the isola with W_S.) Thus the second mechanism yields a disconnected image of a connected curve from the halfplane S^-.

Still, the first cutting open mechanism is found on all complicated isolae as well. It behaves locally similarly to the one discussed above: Adjacent points of the isola, to the left and right of s_1 in Fig. 3b, are mapped to opposite ends of the image on the corresponding base line. In contrast to the "pure" first mechanism, however, here, when approaching the second cutting open point (s_2) in a counter-clockwise manner and the intersection point of the isola in question with W_S (the image of s_2) in a clockwise manner, the two images coalesce (are glued together) in the "middle" of the base line (see [2], Figure 10). The geometric locus of "gluing together points" was found numerically in [6] and called a "hook". It turns out that these curves possess an interesting dynamics themselves, one that is strongly related both to that of the critical spiral and to that of the "return-transfer boundary" discussed in [8] (work submitted [11]).

The *third* and last separating mechanism (type III) yields a combination of the first two and was described analytically here for the first time. It appears together with doubly touching trajectories when the critical spiral becomes capable of crossing W (as occurs above the curve Ω_1 in parameter space). In this case specific selection rules had to be introduced in order to select those portions of the spiral that contribute to the halfmap. These rules cut out segments of the spiral and thereby eliminate those mapping times where no separation occurs.

While the first separating mechanism affects all isolae and a portion of the Ω-curves, and the second one acts only on the complicated isolae, the third mechanism is restricted even further. It interferes only with those isolae that harbor self-intersection points of the critical spiral. At these points *three* different regions of the halfplane S^- meet, being mapped far apart from each other. This latter mechanism, together with the second one, gains more and more importance for higher frequencies of the saddle-focus. Then a greater portion of the family of isolae

becomes complicated and, moreover, every time a further Ω_n curve is crossed, a new path is opened for an additional doubly touching trajectory to occur.

By quantitatively characterizing the critical spiral, it was possible to obtain a complete and unified description of the separating (or "cutting open", respectively) mechanisms that occur in Poincaré halfmaps. Hence the different kinds of chaotic solutions to be found in piecewise-linear continuous, autonomous 3-D dynamical systems may be characterized in terms of the separating mechanisms that are used recursively by the overall dynamics, i.e., the combination of both halfmaps [12].

Apart from the separating mechanisms, discussed here, we expect chaos also to arise due to "folding type divergencies" [10] in the halfmap. A detailed discussion of this "weakest" chaos-generating mechanism is also in preparation [13].

To conclude, the dynamical behavior of piecewise-linear systems can be analyzed further. While in general only implicit equations are obtained it unexpectedly turned out that these implicit equations permit explicit expressions for many properties of interest.

Appendix

A Lemma from Analysis: *For values of the parameters $\sigma, \omega > 0$ the function*

$$F(t) = -\omega + e^{-\sigma t}(\omega \cos \omega t + \sigma \sin \omega t) \quad \text{(A. 1)}$$

possesses its only nonnegative zero at $t = 0$. □

Proof: We show that the zero at $t = 0$ is the greatest maximum possible for $t \geqq 0$: The derivative of F reads

$$F'(t) = -(\omega^2 + \sigma^2)\, e^{-\sigma t} \sin \omega t. \quad \text{(A. 2)}$$

This means that the extrema t_n of F coincide with the zeros of the sine function. At $t = 0$ a maximum is found since the second derivative there.

$$F''(0) = -\omega(\omega^2 + \sigma^2), \quad \text{(A. 3)}$$

is a negative quantity. To show that this is the greatest of all nonnegative maxima, we just have to keep in mind that the amplitude, $e^{-\sigma t}$, of the oscillatory term in F, is strictly decreasing. Hence at all the subsequent maxima of F the second term is smaller by a factor $e^{-2\pi\sigma/\omega}$ than the preceding one. The sequence of maxima of F is thus

$$F(t_n) = \omega(-1 + e^{-2\pi n\sigma/\omega}); \quad n = 0, 1, 2 \ldots . \quad \text{(A. 4)}$$

Therefore the constant term $-\omega$ in F is only at $t = 0$ compensated by the damped oscillatory term. □

The above Lemma applies directly to z as well as to n, by putting $\sigma = 1$ or $\sigma = (\varrho + 1)$, respectively.

Acknowledgement

This work was supported by the DFG.

[1] C. Kahlert, Z. Naturforsch. **41 a,** 567 (1986).
[2] C. Kahlert and O. E. Rössler, Z. Naturforsch. **40 a,** 1011 (1985). Equation (64) of this paper should read $r_C = \eta_\infty \varrho (\varrho + 1)^{-(\varrho+1)/\varrho}$.
[3] C. Kahlert and O. E. Rössler, Z. Naturforsch. **38 a,** 648 (1983).
[4] D. Ruelle, Sensitive dependence on initial conditions and turbulent behavior of dynamical systems, in Bifurcation Theory and its Applications in Scientific Disciplines, O. Gurel and O. E. Rössler, Editors, Ann. New York Acad. Sci. **316,** 408 (1979).
[5] P. Grassberger and I. Procaccia, Phys. Rev. Lett. **50,** 346 (1983).
[6] B. Uehleke and O. E. Rössler, Z. Naturforsch. **38 a,** 1107 (1983).
[7] C. Kahlert, Infinite Nonperiodic Wavetrains in a Class of Reaction-Diffusion-Equations – Analytical Properties of Poincaré Halfmaps (in German), Ph. D. Thesis, University of Tübingen, 1984.
[8] C. Kahlert and L. O. Chua, Transfer maps and return maps for piecewise-linear three-region dynamical systems, International Journal of Circuit Theory and Applications, **14** (1986), in press.
[9] E. C. Titchmarsh, Theory of Functions, University Press, Oxford 1939.
[10] O. E. Rössler, Z. Naturforsch. **31 a,** 1664 (1976).
[11] C. Kahlert, Inverse Poincaré halfmaps, submitted to Z. Naturforsch. 1986.
[12] C. Kahlert, The composition of Poincaré halfmaps and chaotic attractors, in preparation.
[13] C. Kahlert and O. E. Rössler, The formation of Smale Horseshoes in composite Poincaré halfmaps, in preparation.